Progress In Electromagnetics Research M, Vol. 70, 81–88, 2018

A Compact QMSIW CSRR Bandpass Filter with Simultaneous Size Reduction and Improved Wide Stopband

Li Sun, Guo-Hui Li*, Ya-Na Yang, Wei Yang, and Xue-Xia Yang

Abstract—A size-reduced quarter-mode substrate integrated waveguide (QMSIW) band-pass filter (BPF) loaded with combination of complementary split ring resonator (CSRR) and capacitive metal patches is presented. The CSRR generates a passband below the characteristic cutoff frequency of the substrate integrated waveguide (SIW) cavity. Improved stopband rejection is also attainable by loading a capacitive metal patch. Thus, a single-layer compact BPF with wide stopband is realized successfully. The equivalent-circuit model has been derived and analyzed. To verify the validity of the presented method, an experimental filter centered at 2.45 GHz is fabricated and measured. The new filter has the return loss of 16 dB and insertion loss less than 0.9 dB. Out-of-band suppression is better than 20 dB from 3 GHz to 11.6 GHz. The whole size of the filter is only $20 \times 17.4 \times 0.508\,\text{mm}^3$, achieving 75% size reduction compared to the conventional structure.

1. INTRODUCTION

With the rapid development of communication technology, it is imperative to develop size-reduced filter with wide stopband, high selectivity, easy integration, low cost, etc. Substrate integrated waveguide (SIW) is one kind of ideal waveguide that can be manufactured using via-hole in a conventional dielectric substrate, while preserving most of the advantages of rectangular waveguide. It has been widely applied to design filter due to its high Q factor, low cost and convenient integration with other electronic components [1]. However, the volume of the filter designed by the traditional SIW structure is still too large to integrate with microsystem. Recently, half-mode SIW (HMSIW) [2] and quarter-mode SIW (QMSIW) [3] have been proposed to reduce the filter dimension about 50% and 75%. Other researches show that CSRR have excellence property of generating forward wave transmission below the waveguide cutoff frequency [4, 5]. Moreover, the intrinsic resonance frequency of the CSRR can be electronically tuned by adding variable capacitors to the inner conductors since CSRR behaves as a resonant LC tank [6]. Furthermore, it is easy to etch the CSRR on waveguide surface of QMSIW. The miniaturized design is further enhanced by combining QMSIW with CSRR. So far, several techniques have been described to miniaturize the filters, such as HMSIW with defected ground structure (DGS) [7] and multi-layer SIW filter technology [8]. Techniques for improving the stopband performance of multi-layer substrate integrated waveguide filter have been described in [9].

In order to obtain filter with small size, a compact QMSIW band-pass filter loaded by CSRR and a capacitive metal patch is proposed in this paper. First, a compact QMSIW-CSRR band-pass filter is designed by analyzing the dimension of CSRR and equivalent circuit. Then a capacitive metal patch is loaded on the QMSIW-CSRR cavity to achieve the wide stopband. The wide stopband filter is completed using the full-wave EM simulator software (Ansoft HFSS 15). Finally, a filter prototype bandpass filter centered at 2.45 GHz with small circuit size is manufactured and measured on Rogers RT/Duroid 5880 substrate.

Received 6 April 2018, Accepted 24 June 2018, Scheduled 5 July 2018

* Corresponding author: Guo-Hui Li (shghlee@163.com).

The authors are with the Key Laboratory of Specialty Fiber Optics and Optical Access Network, Shanghai University, Shanghai 200072, China.

2. ANALYSIS AND DESIGN OF FILTER

2.1. Design of QMSIW-CSRR Filter

To reduce the size of the SIW devices, the HMSIW is proposed by bisecting the SIW along a fictitious magnetic wall. The HMSIW can offer low radiation and insertion loss (IL) while preserving the field distribution of the original SIW. The HMSIW can be further divided into two parts again along the symmetrical plane. The field distribution of the QMSIW is same as that of the SIW. Fig. 1 presents the comparison of the electric field distribution for the SIW cavity and the QMSIW cavity. It is obvious that the QMSIW structure offers a new concept to design compact filters.

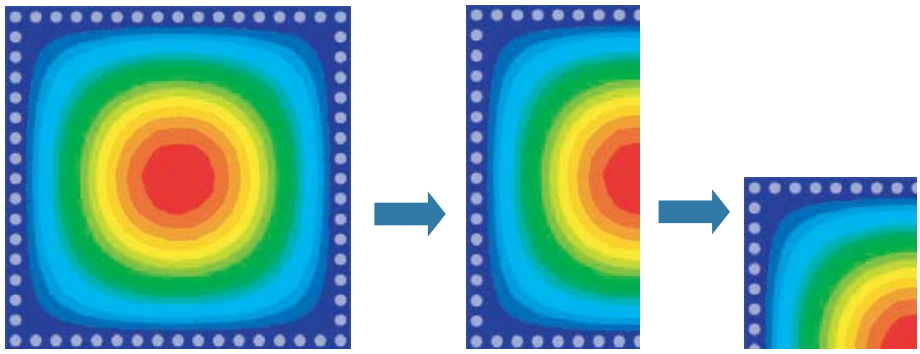

Figure 1. Electric field distributions for rectangle. (a) SIW cavity. (b) HMSIW cavity. (c) QMSIW cavity.

In QMSIW structure, the resonant frequency of TE_{101} can be calculated by the formula [10].

$$f_{TE_{101}}^{QMSIW} = \frac{c}{2\pi\sqrt{\mu_r\varepsilon_r}}\sqrt{\left(\frac{\pi}{a_{eff}^{QMSIW}}\right)^2 + \left(\frac{\pi}{a_{eff}^{QMSIW}}\right)^2} \tag{1}$$

where a_{eff}^{QMSIW} is the equivalent length of the QMSIW cavity; c is the light speed in free space; μ_r and ε_r are the relative permeability and permittivity of the cavity substrate.

The coupling mechanism investigated in this paper is side coupling [11]. As shown in Fig. 2(a), two uncoupled quarter-mode resonators share a post wall and then an aperture is created by removing

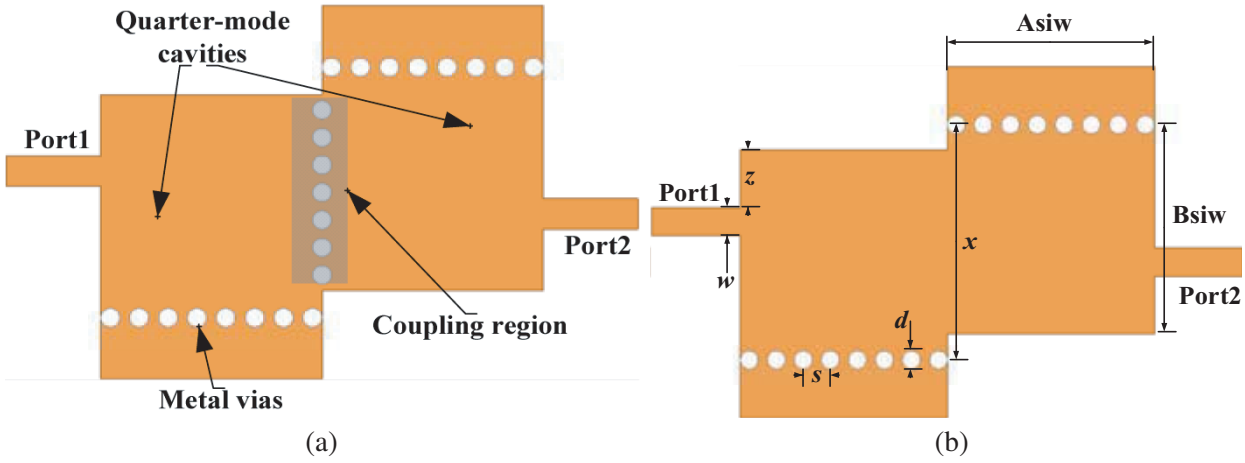

Figure 2. (a) Two separated quarter-mode SIW cavities. (b) Basic geometry of the QMSIW filter.

some posts. The side coupling is obtained by laterally shifting the resonators of a quantity x, which will lead to a change of the aperture size. The basic structure of filter is shown in Fig. 2(b), where $Asiw = 7\,\text{mm}$, $Bsiw = 7\,\text{mm}$, $x = 8.6\,\text{mm}$, $z = 3\,\text{mm}$. The simulated S-parameters of QMSIW filter are shown in Fig. 3.

The combination of CSRRs and SIW is illustrated to design the miniaturized bandpass filters when a forward-wave passband propagates below the characteristic cutoff frequency of the waveguide [4]. In this study, the filter structure and LC equivalent circuit model are shown in Fig. 4, where two CSRRs are etched on the upper metallic surface of QMSIW cavity respectively. Because the electric field is perpendicular to the metal surfaces in the QMSIW cavity, new resonant frequency can be generated by changing the shape of the upper metallic surface. According to CSRR, the electrical equivalent circuit of the QMSIW-CSRR filter is shown in Fig. 4(b), in which the resonant tank formed by L_{s1} and C_{s1} models the coupling between source and the first cavity, whereas L_{2L} and C_{2L} represent the coupling between load and the second cavity. The effect of the CSRR is modeled as a series resonant tank formed by L_{r1}, C_{r1}, L_{r2} and C_{r2}, while the inductance L_{d1} and L_{d2} describe the inductive effect of

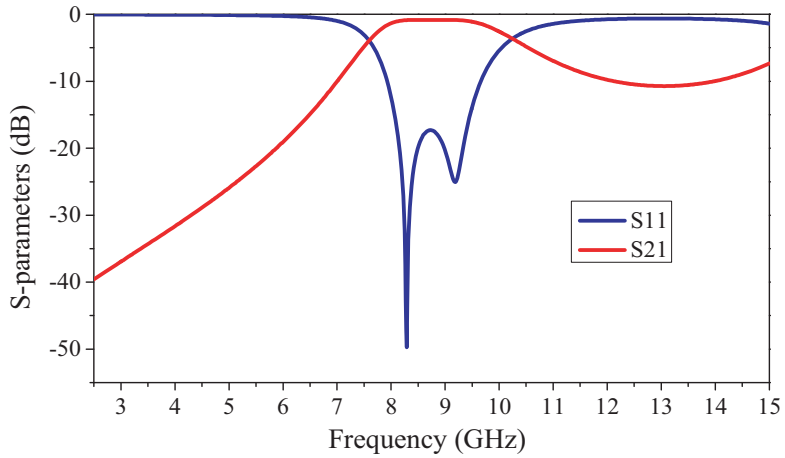

Figure 3. The simulated S-parameters of QMSIW filter.

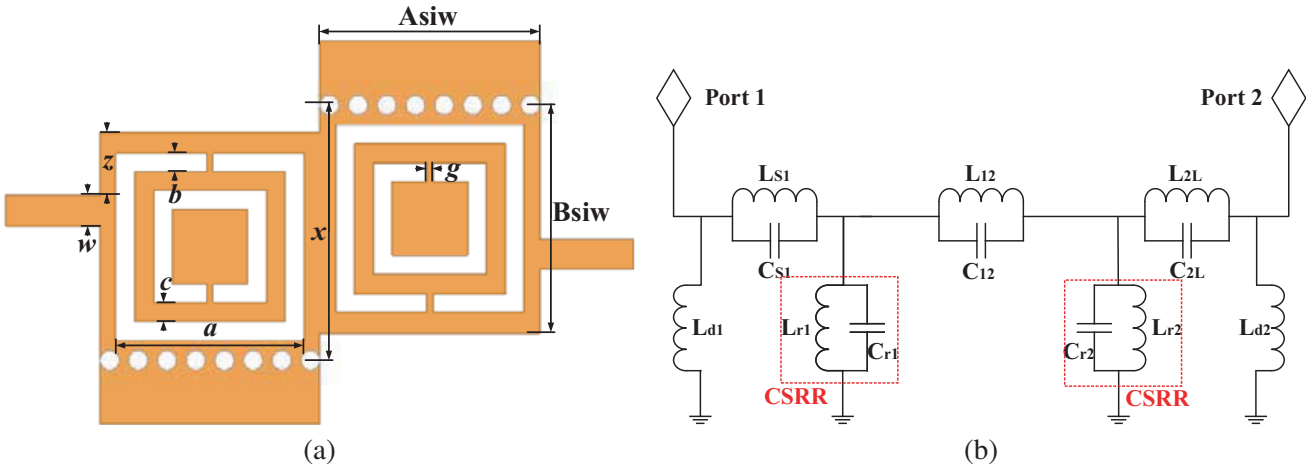

Figure 4. (a) Structure of QMSIW-CSRR filter. The dimension parameters are $a = 6\,\text{mm}$, $b = 1\,\text{mm}$, $c = 1\,\text{mm}$, $g = 0.2\,\text{mm}$, $w = 1\,\text{mm}$, $z = 1\,\text{mm}$, $Asiw = 7\,\text{mm}$, $Bsiw = 7\,\text{mm}$. (b) The equivalent circuit of the QMSIW-CSRR filter. The extracted equivalent circuit parameters are $L_{s1} = 0.903\,\text{nH}$, $C_{s1} = 0.803\,\text{pF}$, $L_{12} = 1.777\,\text{nH}$, $C_{12} = 0.58\,\text{pF}$, $L_{2L} = 0.85\,\text{nH}$, $C_{2L} = 0.85\,\text{pF}$, $L_{d1} = 28\,\text{nH}$, $L_{d1} = 4.318\,\text{nH}$, $L_{r1} = 0.633\,\text{nH}$, $C_{r1} = 4.09\,\text{pF}$, $L_{r2} = 0.653\,\text{nH}$, $C_{r2} = 4.14\,\text{pF}$.

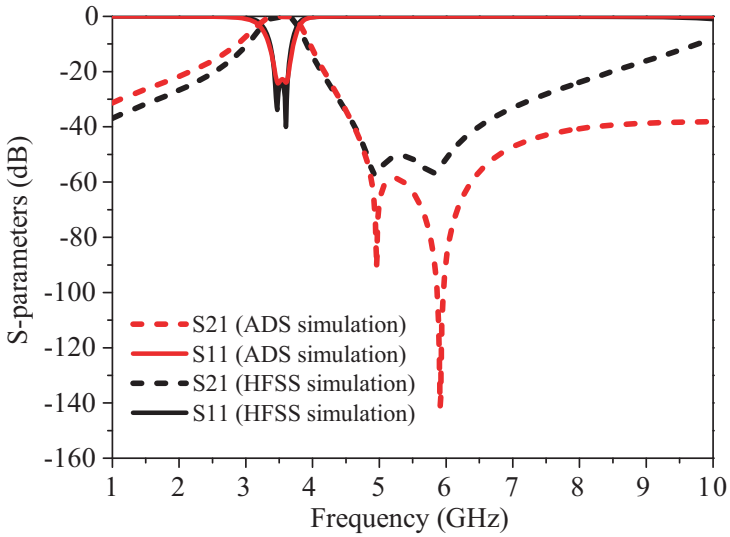

Figure 5. Comparison between the full wave simulation and the equivalent circuit model.

the via wall. Fig. 5 shows the EM simulation (by HFSS) and equivalent circuit (by ADS) results with good agreement. Two transmission zeros can be realized to extend bandwidth of stopband. The major discrepancy appears in the high-frequency range, where the equivalent circuit model presents serious accuracy problems, as shown in Fig. 5. This is especially evident for the S_{21} parameter. The difference is due to the inaccuracy of the equivalent circuit model in higher frequency regions. From the above analysis, it is clear that equivalent circuit that we propose in this paper is acceptable in the frequency range of our interests for the QMSIW-CSRR filter. It is explicitly observed that the size of CSRR is determined by a, b, c and g, where a represents the side length of the outer ring, b the strip width of the resonant ring, c the separation between two adjacent rings, and g the length of the split. The equivalent circuit of CSRR structure can be regarded as a parallel LC tank. Its resonant frequency is calculated by the following formula:

$$f_{CSRR} = \frac{1}{2\pi\sqrt{L_{CSRR}C_{CSRR}}} \tag{2}$$

where L_{CSRR} and C_{CSRR} denote the effective inductance and equivalent capacitance of CSRR, respectively. The resonant frequency of CSRR can be adjusted by changing the size of a, b, c and g. The concrete relationship between dimension and resonant frequency is illustrated as follows: the corresponding resonant frequency moves to lower frequency as a increases, shown in Fig. 6(a); the resonant frequency increases when b or c or g increases, shown in Fig. 6(b), Fig. 6(c) and Fig. 6(d), respectively.

2.2. Design of QMSIW-CSRR Filter with Wide Stopband

As an illustrative example, a compact filter is obtained by loading capacitive metal patches on QMSIW-CSRR. Fig. 7 shows the configuration of the capacitive-loaded QMSIW-CSRR filter. It is found that the wide stopband performance is realized by loading capacitive metal patches on the cavity, as shown in Fig. 8(a). Note that center frequency shifts to lower frequency when n increases and a spurious resonant mode occurs in the upper stopband with an improper n. From Fig. 8(b), it can be concluded that the stopband characteristic is significantly affected by gs, but the center frequency is hardly influenced by gs. Hence, the center frequency is determined by choosing the proper dimensions. An appropriate gs is optimized to eliminate the spurious resonant mode. The dimension parameters are adopted after optimization as follows: $a = 6.4\,\text{mm}$, $b = 0.6\,\text{mm}$, $c = 1\,\text{mm}$, $g = 0.2\,\text{mm}$, $w = 1\,\text{mm}$, $l = 3\,\text{mm}$, $z = 1\,\text{mm}$, $Asiw = 7\,\text{mm}$, $Bsiw = 7\,\text{mm}$, $m = 6\,\text{mm}$, $n = 5\,\text{mm}$, $gs = 0.2\,\text{mm}$.

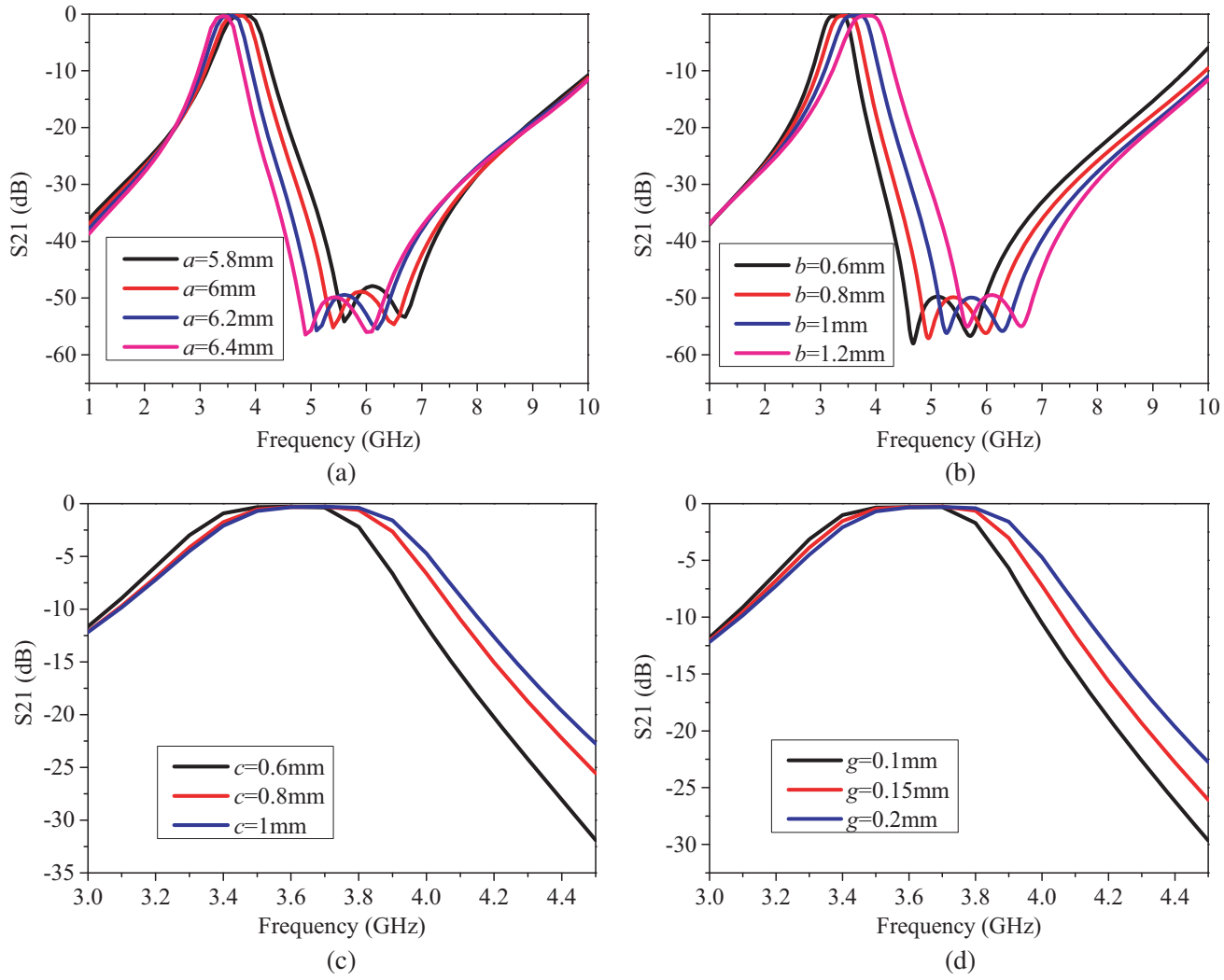

Figure 6. The simulated S_{21} with different values of a, b, c and d.

3. FABRICATION AND MEASUREMENT

To validate the simulated filtering performance, a compact filter is fabricated on a Rogers 5880 substrate with $\varepsilon_r = 2.2$ and height of 0.508 mm. Fig. 9(a) shows the photograph of the fabricated filter. The circuit size of the prototype filter is $20 \times 17.4\,\text{mm}^2$, i.e., $0.24 \times 0.21\lambda g^2$, where λg is the guided wavelength

Table 1. Comparison between the proposed filter and the literatures.

	f_0 (GHz)	IL (dB)	RL (dB)	Stopband width (> 20 dB)	Size $\lambda_g \times \lambda_g$
[12]	5.57	2	18.1	$1.38f_0$	0.42×0.42
[13]	5	2.1	16	$2.1f_0$	-
[14]	8.5	1.1	11	$0.55f_0$	1.25×0.63
[15]	4.9	1.1	17	$0.54f_0$	0.39×0.39
[16]	3.5	1.45	15	$0.6f_0$	0.4×0.44
This work	2.45	0.9	16	$3.51f_0$	0.24×0.21

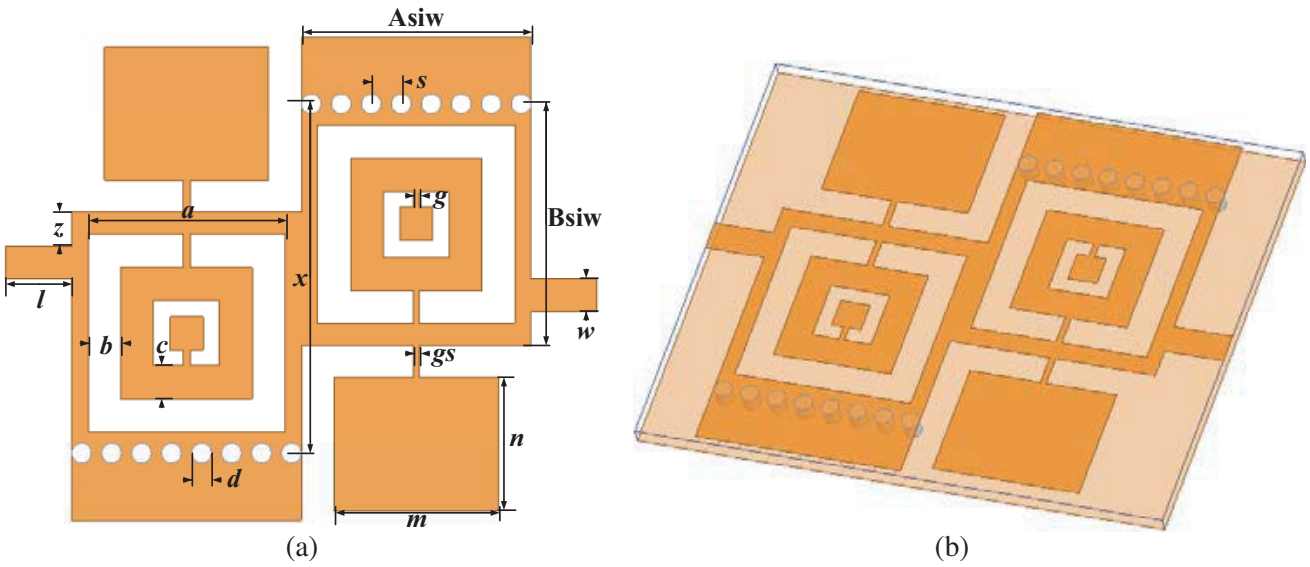

Figure 7. Configuration of the proposed filter. (a) Top view. (b) 3-D graph.

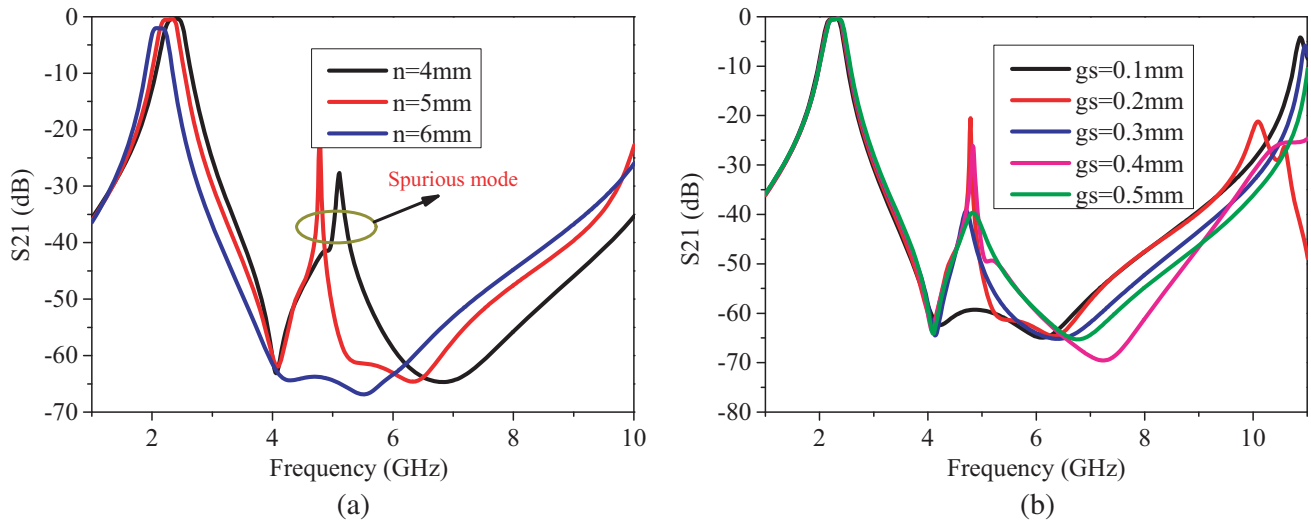

Figure 8. Frequency responses of filter with various (a) n, (b) gs.

at the center frequency. The fabricated filter was measured using Agilent 8722ES network analyzer.

Figure 9(b) presents a comparison between the measured and simulated scattering parameters of the fabricated filter. As can be seen, the 3-dB fractional bandwidth is 17.1%. Within the passband, the measured RL is better than 16 dB, and the insertion loss is approximately 0.9 dB at the central frequency of 2.45 GHz. In addition, the FBW of the filter is 17.1%. In the upper band, stopband rejection better than 20 dB across a range from 3 GHz to 11.6 GHz is obtained. It should be pointed out that a slight difference in RL and IL between simulated and measured results is observed, which is mainly attributed to the loss of SMA connector and filter manufacture precision.

Table 1 summarizes the comparison between the proposed filter and some reported filters. It is shown that the IL in this work is minimum close to 0.9 dB. Though RL of the proposed filter is 16 dB smaller than that of [12], better stopband width and small size are achieved. It can be found that this filter has advantages of small insertion loss, extremely compact size and wide stopband in spite of its relatively small RL. Therefore, overall performances of the proposed filter are better than those of others.

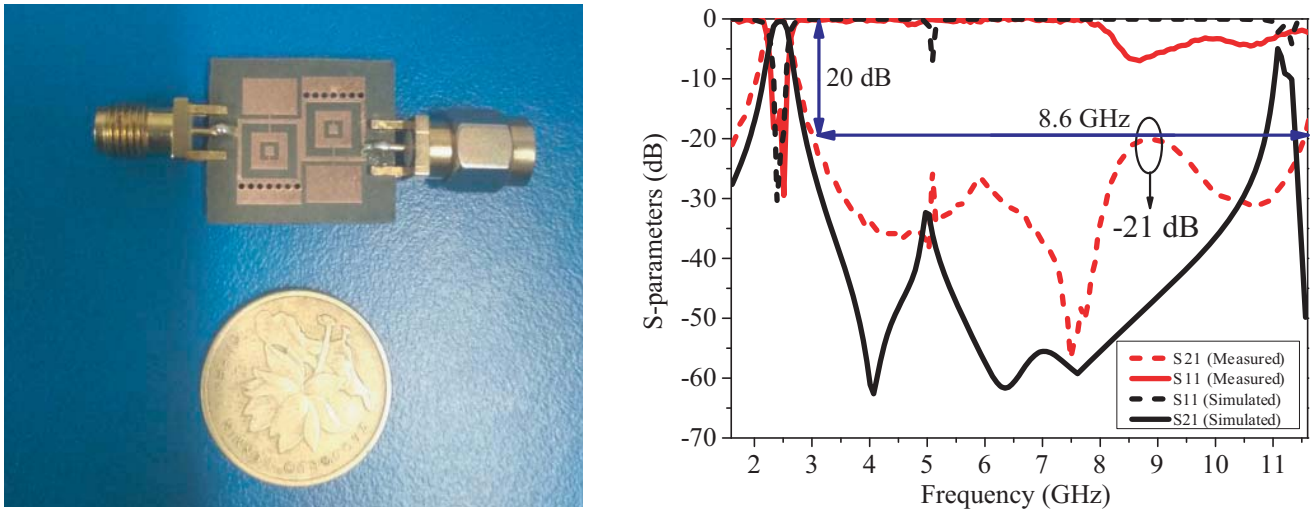

Figure 9. (a) Photograph of the fabricated filter. (b) Simulated and measured S-parameters.

4. CONCLUSION

In this paper, the design and measurement of compact QMSIW bandpass filter loaded with CSRR and capacitance is presented. The capacitively-loaded CSRR QMSIW structure not only allows for miniaturization up to more than 75% compared to conventional SIW, but also achieves wider stopband, while still maintaining lower IL and high RL. The wide stopband performance of 20-dB suppression is from 3 GHz to 11.6 GHz, about $3.51f_0$. The oversize of the filter is only $0.24\lambda g \times 0.21\lambda g$. The measured values are somewhat worse than simulation ones, but the result indicates that the proposed filter can be a potential candidate for Radio Frequency Identification systems.

REFERENCES

1. Huang, L. and H. Cha, "Compact ridge substrate integrated waveguide filter with transmission zeros," *IEEE Microw. Wireless Compon. Lett.*, Vol. 25, No. 12, 778–780, 2015.
2. Wang, Y., W. Hong, Y. Dong, B. Liu, H.-J. Tang, J. Chen, X. Yin, and K. Wu, "Half mode substrate integrated waveguide (HMSIW) band-pass filter," *IEEE Microw. Wireless Compon. Lett.*, Vol. 17, No. 4, 265–267, 2007.
3. Zhang, Z., N. Yang, and K. Wu, "5-GHz bandpass filter demonstration using quarter-mode substrate integrated waveguide cavity for wireless systems," *2009 IEEE Radio and Wireless Symposium (RWS)*, 18–22, 2009.
4. Dong, Y.-D., T. Yang, and T. Itoh, "Substrate integrated waveguide loaded by complementary split-ring resonators and its applications to miniaturized waveguide filters," *IEEE Trans. Microw. Theory Tech.*, Vol. 57, No. 9, 2211–2223, 2009.
5. Khan, S. N., X. Liu, L. Shao, and Y. Wang, "Complementary split ring resonators of large stop bandwidth," *Progress In Electromagnetics Research Letters*, Vol. 14, 127–132, 2010.
6. Senior, D. E., X. Cheng, and Y.-K. Yoon, "Electrically tunable evanescent mode half-mode substrate-integrated-waveguide resonators," *IEEE Microw. Wireless Compon. Lett.*, Vol. 22, No. 3, 123–125, 2012.
7. Yang, Z., Z. Wang, J. Dong, J. Liu, and T. Yang, "Compact wideband HMSIW bandpass filter with defected ground structure," *2015 IEEE International Conference on Signal Processing, Communications and Computing (ICSPCC)*, 1–4, 2015.

8. Khalil, M., M. Kamarei, and J. Jomaah, "Compact multi-layer band-pass filter in Substrate Integrated Waveguide (SIW) technology," *2016 IEEE Middle East Conference on Antennas and Propagation (MECAP)*, 1–4, 2016.
9. Jia, D., Q. Feng, Q. Xiang, and K. Wu, "Multilayer Substrate Integrated Waveguide (SIW) filters with higher-order mode suppression," *IEEE Microw. Wireless Compon. Lett.*, Vol. 26, No. 9, 678–680, 2016.
10. Li, P., H. Chu, and R.-S. Chen, "Design of compact bandpass filters using quarter-mode and eighth-mode SIW cavities," *IEEE Trans. Compon. and Packag. Tech.*, Vol. 7, No. 6, 956–963, 2017.
11. Moscato, S., C. Tomassoni, M. Bozzi, and L. Perregrini, "Quarter-mode cavity filters in substrate integrated waveguide technology," *IEEE Trans. Microw. Theory Tech.*, Vol. 64, No. 8, 2538–2547, 2016.
12. Guo, Z., K. S. Chin, W. Che, and C.-C. Chang, "Cross-coupled band-pass filters using QMSIW cavities and S-shaped slot coupling structures," *Journal of Electromagnetic Waves and Applications*, Vol. 27, No. 2, 160–167, 2013.
13. Shen, W., W.-Y. Yin, X.-W. Sun, and J.-F. Mao, "Compact coplanar waveguide-incorporated Substrate Integrated Waveguide (SIW) filter," *Journal of Electromagnetic Waves and Applications*, Vol. 24, No. 7, 871–879, 2010.
14. Chen, R.-S., S.-W. Wong, L. Zhu, and Q.-X. Chu, "Wideband bandpass filter using U-slotted Substrate Integrated Waveguide (SIW) cavities," *IEEE Microw. Wireless Compon. Lett.*, Vol. 25, No. 1, 1–3, 2015.
15. Shen, W., W.-Y. Yin, and X.-W. Sun, "Compact Substrate Integrated Waveguide (SIW) filter with defected ground structure," *IEEE Microw. Wireless Compon. Lett.*, Vol. 21, No. 2, 83–85, 2011.
16. Zhang, Q.-L., W.-Y. Yin, S. He, and L.-S. Wu, "Compact Substrate Integrated Waveguide (SIW) bandpass filter with Complementary Split-Ring Resonators (CSRRs)," *IEEE Microw. Wireless Compon. Lett.*, Vol. 20, No. 8, 426–428, 2010.